Alternative sulfonylurea receptor expression defines metabolic sensitivity of K-ATP channels in dopaminergic midbrain neurons

Birgit Liss, Ralf Bruns and Jochen Roeper[1,2]

Institute for Neural Signal Transduction, Centre for Molecular Neurobiology, Martinistraße 52, 20246 Hamburg, Germany

[1]Present address: MRC Anatomical Neuropharmacology Unit, Oxford University, Mansfield Road, Oxford OX1 3TH, UK

[2]Corresponding author
e-mail: roeper@plexus.uke.uni-hamburg.de

R.Bruns contributed experiments shown in Figure 6C and D

ATP-sensitive potassium (K-ATP) channels couple the metabolic state to cellular excitability in various tissues. Several isoforms of the K-ATP channel subunits, the sulfonylurea receptor (SUR) and inwardly rectifying K channel (Kir6.X), have been cloned, but the molecular composition and functional diversity of native neuronal K-ATP channels remain unresolved. We combined functional analysis of K-ATP channels with expression profiling of K-ATP subunits at the level of single substantia nigra (SN) neurons in mouse brain slices using an RT–multiplex PCR protocol. In contrast to GABAergic neurons, single dopaminergic SN neurons displayed alternative co-expression of either SUR1, SUR2B or both SUR isoforms with Kir6.2. Dopaminergic SN neurons expressed alternative K-ATP channel species distinguished by significant differences in sulfonylurea affinity and metabolic sensitivity. In single dopaminergic SN neurons, co-expression of SUR1 + Kir6.2, but not of SUR2B + Kir6.2, correlated with functional K-ATP channels highly sensitive to metabolic inhibition. In contrast to wild-type, surviving dopaminergic SN neurons of homozygous *weaver* mouse exclusively expressed SUR1 + Kir6.2 during the active period of dopaminergic neurodegeneration. Therefore, alternative expression of K-ATP channel subunits defines the differential response to metabolic stress and constitutes a novel candidate mechanism for the differential vulnerability of dopaminergic neurons in response to respiratory chain dysfunction in Parkinson's disease.
Keywords: ATP-sensitive potassium channel/Parkinson's disease/single-cell RT–PCR/substantia nigra/weaver

Introduction

Chronic metabolic stress is believed to play an important role in neurodegenerative disorders such as Parkinson's or Huntington's disease (Beal, 1996; Hanna and Bhatia, 1997). Different neuronal populations are not affected equally by metabolic challenges (Schreiber and Baudry, 1995), and resistant subpopulations within degenerating nuclei have been identified (Hirsch *et al*., 1997). Therefore, it is of considerable interest to define the molecular basis of differential neuronal vulnerability. Neuronal ATP-sensitive potassium (K-ATP) channels might be one of the promising targets acting as direct functional response elements to metabolic stress (Roeper and Ashcroft, 1995; Trapp and Ballanyi, 1995; Fujimura *et al*., 1997). K-ATP channels couple membrane excitability to cellular metabolism by directly sensing and integrating intracellular concentration changes of nucleotides such as ATP and ADP (Ashcroft, 1988; Quale *et al*., 1997; Aguilar-Bryan *et al*., 1998; Babenko *et al*., 1998; Yokoshiki *et al*., 1998).

Sulfonylurea binding and electrophysiological studies have characterized neuronal K-ATP channels with different properties in a variety of cell types, including hippocampal CA1 neurons, dorsal vagal neurons and hypothalamic neurons (Trapp and Ballanyi, 1995; Dunn-Meynell *et al*., 1997; Fujimura *et al*., 1997; Spanswick *et al*., 1997). We and others have identified functional somatodendritic K-ATP channels on dopaminergic substantia nigra (SN) pars compacta neurons. These neuronal K-ATP channels were activated by different paradigms of metabolic stress such as hypoxia, sodium loading, glucose removal or dialysis with ATP-free pipette solutions (Mercuri *et al*., 1994; Roeper and Ashcroft, 1995; Watts *et al*., 1995; Seutin *et al*., 1996; Stanford and Lacey, 1995). We have shown previously that inhibition of mitochondrial complex I by rotenone leads to a tonic activation of K-ATP channels, complete cessation of spontaneous electrical activity and membrane hyperpolarization in dopaminergic SN neurons (Roeper and Ashcroft, 1995). This is of particular interest, as complex I inhibition is one of the proposed trigger mechanisms of degeneration of dopaminergic midbrain neurons in Parkinson's disease (Beal, 1996; Hanna and Bhatia, 1997; Hirsch *et al*., 1997).

The cloning of K-ATP channel subunits (Aguilar-Bryan *et al*., 1995; Sakura *et al*., 1995; Chutkow *et al*., 1996; Inagaki *et al*., 1995a, 1996) allowed us to probe for the molecular identity of neuronal K-ATP channels in SN neurons. K-ATP channels are heterooligomeric proteins composed of two types of subunits, a sulfonylurea receptor (SUR) and an inwardly rectifying K channel subunit (Kir6.X), which assemble in a 4:4 stoichiometry (Clement *et al*., 1997). Two related isoforms of the SUR have been identified, SUR1 and SUR2; the latter exists in at least two alternatively spliced forms (SUR2A and SUR2B) (Chutkow *et al*., 1996; Inagaki *et al*., 1996; Isomoto *et al*., 1996; Yamada *et al*., 1997). In addition, two related Kir6.X channels have been identified, Kir6.1 and Kir6.2 (Inagaki *et al*., 1995b; Sakura *et al*., 1995). Co-expression experiments of different SUR and Kir6 isoforms in heterologous systems suggested that different functional properties and pharmacological profiles of recombinant K-ATP channels are mediated by alternative subunit combinations (Inagaki *et al*., 1996; Isomoto *et al*., 1996; Gribble *et al*., 1997; Yamada *et al*., 1997; Okuyama *et al*., 1998).

B.Liss, R.Bruns and J.Roeper

The aim of this study was to identify the molecular composition and functional diversity of native K-ATP channels in midbrain neurons at the level of single cells. In addition to wild-type neurons, we also analysed K-ATP channel expression profiles of dopaminergic SN neurons in the *weaver* mouse, a genetic model of selective degeneration of a subpopulation of dopaminergic SN neurons induced by a pore mutation in a G-protein-activated inwardly rectifiying K channel (Girk2; Graybiel *et al.*, 1990; Bayer *et al.*, 1995; Patil *et al.*, 1995). We combined electrophysiological analysis with single-cell RT–multiplex PCR (RT–mPCR) protocols (Jonas *et al.*, 1994; Monyer and Lambolez, 1995; Audinat *et al.*, 1996; O'Dowd and Smith, 1996; Surmeier *et al.*, 1996; Cauli *et al.*, 1997). In contrast to γ-aminobutyric acid (GABA)ergic SN neurons, single wild-type dopaminergic SN neurons displayed alternative expression profiles of K-ATP channel subunits (SUR1 + Kir6.2 and SUR2B + Kir6.2) and functional K-ATP channels with different pharmacological and metabolic properties. The co-expression of SUR1 + Kir6.2, but not of SUR2B + Kir6.2, was correlated with functional K-ATP channels highly sensitive to complex I inhibition. In addition, surviving dopaminergic SN neurons in homozygous *weaver* mice exclusively expressed SUR1 + Kir6.2.

Results

RT–multiplex PCR

An RT–mPCR protocol (Cauli *et al.*, 1997) was designed simultaneously to detect, at the single-cell level, the mRNAs of the K-ATP channel subunits SUR1, SUR2, Kir6.2 and Kir6.1, as well as the mRNAs for the Girk2 subunit of the G-protein-activated inwardly rectifying K channel (Lesage *et al.*, 1994), and the marker genes tyrosine hydroxylase (TH) (Iwata *et al.*, 1992), glutamate decarboxylase (GAD67) (Szabó *et al.*, 1996) and glial fibrillary acidic protein (GFAP) (Brenner, 1994). The expression profiles of the marker genes were used to classify analysed SN cells as dopaminergic (TH[+]) and GABAergic (GAD67^{+}) neurons, and to exclude astroglial cells (GFAP[+]). Girk2, which is known to be expressed in dopaminergic SN neurons, was included to control the ability to detect low abundance ion channel transcripts in single neurons. For this technique, two rounds of PCR amplification, an initial mPCR and a subsequent nested PCR, were used after reverse transcription. The sensitivity of the protocol was optimized using highly diluted midbrain cDNA to allow reliable simultaneous amplification of all eight transcripts from estimated subfemtomolar transcript concentrations, which is likely to be in the range found in single cells. Figure 1A shows that the eight specific mRNAs were detected, each generating a PCR fragment of the size predicted by its mRNA sequence. The identities of all PCR fragments were verified by subcloning and sequencing or, alternatively, by direct sequencing. Alternative primer pairs were used to differentiate between the two SUR2 isoforms, SUR2A and SUR2B. In contrast to heart, where both splice variants SUR2A and SUR2B were expressed, only SUR2B is present in ventral midbrain (Figure 1B). Similar results were obtained from single-cell RT–mPCR experiments (see below), indicating that the SUR2A subunit which is believed to
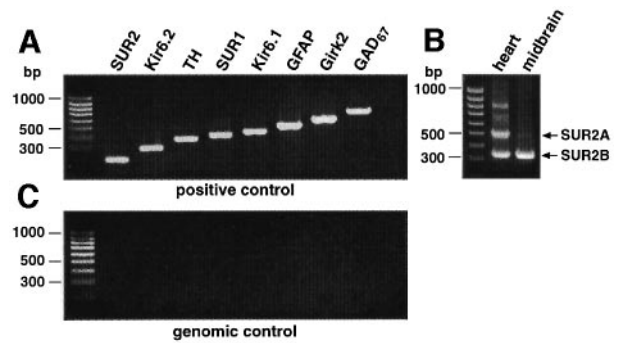

Fig. 1. Sensitivity and specificity of the single-cell multiplex PCR protocol. (**A**) The eight products of nested-PCRs were resolved in separate lanes by agarose gel electrophoresis in parallel with a 100 bp ladder as molecular weight marker and stained with ethidium bromide. Approximately 500 pg of mouse midbrain cDNA was subjected to the mPCR protocol. All four K-ATP channel subunits and the four marker transcripts are expressed in mouse midbrain. The amplified fragments had the size (bp) predicted by the mRNA sequences, and all fragments were verified by sequencing: SUR2 (215), Kir6.2 (298), TH (377), SUR1 (401), Kir6.1 (448), GFAP (517), Girk2 (595) and GAD67 (702). (**B**) Photograph of an ethidium bromide-stained gel with RT–PCR amplicons separated by electrophoresis. PCR fragments were generated with subtype-specific primers for the SUR2 splice variants SUR2A and SUR2B. Note that both SUR2 splice variants were expressed in mouse heart, SUR2A (513 bp) and SUR2B (337 pb), whereas only SUR2B was expressed in ventral midbrain. (**C**) Agarose gel analysis of a single-cell genomic control. Without reverse transcriptase in the reaction, no PCR signal was detected in this and nine other tested neurons.

be one of the components of the cardiac K-ATP channel (Inagaki *et al.*, 1996) is not expressed in SN neurons.

The established single-cell RT–mPCR protocol was then used to analyse the K-ATP channel subunit expression profiles in identified SN neurons. Three different neuronal populations were analysed. Our main interest was focused on the dopaminergic neurons located predominantly in the SN pars compacta (SNpc) (Condé, 1992). For comparison, we also studied a population of small interneurons from the SNpc (Lacey *et al.*, 1989) and GABAergic projection neurons in the SN pars reticulata (SNpr) (Condé, 1992). Recent electrophysiological studies have suggested that two of these neuronal populations, the dopaminergic SNpc (Condé, 1992; Roeper and Ashcroft, 1995; Watts *et al.*, 1995; Seutin *et al.*, 1996; Stanford and Lacey, 1995) and the GABAergic SNpr neurons (Schwanstecher and Panten, 1993; Stanford and Lacey, 1996), possess functional K-ATP channels, whereas the presence of K-ATP channels in SNpc interneurons has not yet been investigated. The different neuronal populations could be identified easily in acute coronal midbrain slices by their morphology and localization within the SN subnuclei. After electrophysiological characterization in the whole-cell patch-clamp mode, the cytoplasm of the cells was harvested carefully under visual control and stable seal conditions for single-cell RT–mPCR. In most cases, the nucleus was also harvested, and the patch pipette repositioned a few times to maximize the cellular yield. To rule out the possibility of genomic contamination by DNA of the single nucleus acting as a potential template for PCR amplification, we performed control single-cell mPCR amplifications without prior reverse transcription, obtaining no detectable PCR products ($n = 10$; Figure 1C). Also, we harvested the cellular contents carefully excluding the nucleus
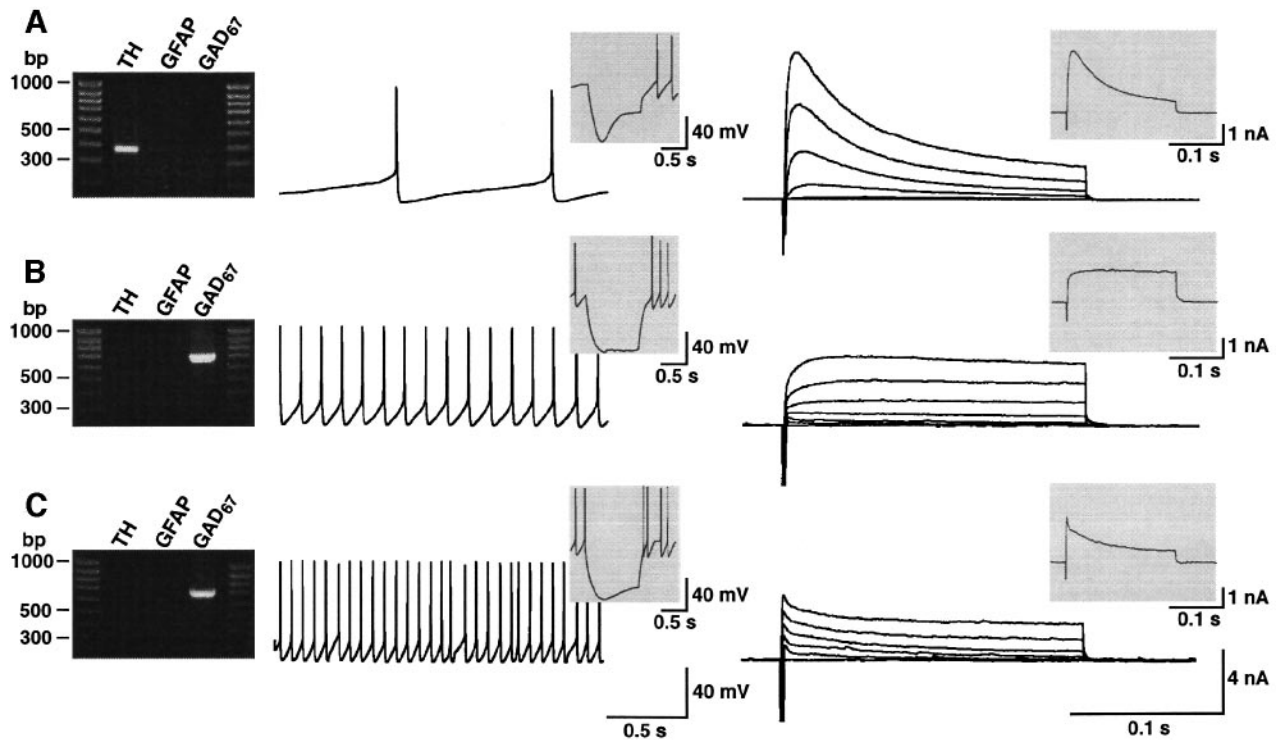
Fig. 2. Electrophysiological properties of substantia nigra neurons with defined molecular phenotypes by single-cell RT–mPCR.
(**A**) Electrophysiological properties of dopaminergic (TH$^+$, GAD67$^-$) SNpc neurons. Current-clamp recordings (left) show spontaneous low frequency pacemaker activity and I_h-mediated response to injection of 100 pA hyperpolarizing current (insert). Voltage-clamp recordings (right) show membrane current responses to 200 ms depolarizing pulses from a holding potential of –80 mV in 10 mV increments to –10 mV. Note the prominent subthreshold A-type current. The insert shows the current response to a depolarization to –30 mV. (**B**) Electrophysiological properties of GABAergic (TH$^-$, GAD67$^+$) SNpc neurons. Current-clamp recordings (left, protocol as in A) shows spontaneous high frequency activity and lack of I_h-mediated sag-response to hyperpolarizing current (insert). Voltage-clamp recordings (right, protocol as in A) show membrane current responses. Note the complete absence of fast inactivating A-type currents. (**C**) Electrophysiological properties of GABAergic (TH$^-$, GAD67$^+$) SNpr neurons. Current-clamp recordings (left, protocol as in A) show high frequency discharge and only a weak sag-response to hyperpolarizing current (insert). Voltage-clamp recordings (right, protocol as in A) show membrane current responses. Note the absence of a prominent subthreshold A-type current.

($n = 5$). After reverse transcription and PCR, we could detect all the cDNAs routinely detected in cells which were harvested, including the nucleus. These control experiments clearly indicate that under our conditions, the genomic DNA of the single nucleus was not acting as a possible template for PCR amplification and that, consequently, we were studying the genuine mRNA expression profiles of single SN neurons.

Electrophysiological properties of substantia nigra neurons with a defined marker expression profile

As expected, the large (30–80 pF) neurons located in the SNpc demonstrated TH, but not GAD67 nor GFAP expression ($n = 77$), indicating their dopaminergic phenotype. At the single-cell level, the TH$^+$ expression profile was correlated consistently with the well-characterized electrophysiological phenotype of dopaminergic SN neurons (Grace and Onn, 1989; Lacey *et al*., 1989; Richards *et al*., 1997) (Figure 2A), i.e. low-frequency pacemaker activity (1.8 ± 0.1 Hz, $n = 70$), broad action potentials (8.0 ± 0.5 ms, $n = 40$), with depolarized thresholds (–36.3 ± 0.8 mV, $n = 40$) and the presence of a strong I_h-dependent sag-current component. In addition, our voltage-clamp analysis of SN neurons showed that a dominant A-type current was found in all cases in TH$^+$ SN neurons ($n = 77$), but was not observed in TH$^-$, GAD67$^+$, i.e. GABAergic SN neurons ($n = 22$). The small interneurons of the SNpc (10–25 pF) showed a marker expression

profile (TH$^-$, GAD67$^+$, GFAP$^-$; $n = 11$) indicating their previously only presumed GABAergic phenotype (Lacey *et al*., 1989; Johnson and North, 1992). These neurons were either electrically silent or displayed spontaneous discharge with higher frequencies compared with TH$^+$ SNpc neurons (8.8 ± 0.6 Hz, $n = 10$; Figure 2B). In voltage-clamp experiments, they possessed no fast-inactivating outward component in the subthreshold range and showed slowly activating outward currents at higher membrane potentials (Figure 2B). The medium sized (20–40 pF) neurons of the SNpr possessed a marker expression profile (TH$^-$, GAD67$^+$, GFAP$^-$; $n = 11$) identifying them as GABAergic. In accordance with previous reports (Richards *et al*., 1997), these SNpr neurons showed either high frequency discharge (11.4 ± 0.7 Hz, $n = 10$) or were electrically silent (Figure 2C). In voltage-clamp, these neurons also lacked a subthreshold A-type current but showed a small, fast-inactivating outward current component at more depolarized potentials (Figure 2C). Girk2 transcripts, which code for one subunit of the G-protein-activated Kir channels, were detected in all dopaminergic ($n = 77$) and GABAergic SNpc neurons ($n = 11$), but only in seven of 11 GABAergic SNpr neurons.

Expression of K-ATP channel subunits in single GABAergic SN neurons

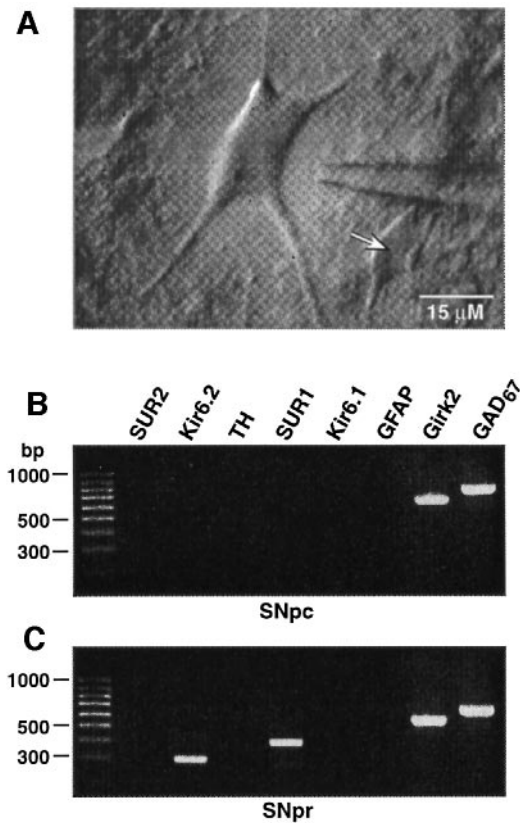Electrophysiological studies reported the presence of functional K-ATP channels on SNpr neurons of unknown

Fig. 3. Homogeneous expression profiles of K-ATP channel subunits in two populations of GABAergic SN neurons revealed by single-cell RT–mPCR. (**A**) IR-DIC videomicroscopy of SNpc neurons in a midbrain slice. Note the large dopaminergic neuron (central) and the smaller GABAergic interneuron (arrow). (**B**) mPCR expression profiling of single GABAergic (TH⁻, GAD67⁺) SNpc neurons. Two PCR products were detected with agarose gel analysis, corresponding to Girk2 (595 bp) and GAD67 (702 bp). No PCR fragments corresponding to any of the tested K-ATP channel subunits were detected in this and 10 other tested GABAergic SNpc neurons. (**C**) mPCR expression profiling of single GABAergic (TH⁻, GAD67⁺) SNpr neurons. Four PCR products were detected corresponding to the K-ATP channel subunits SUR1 (401 bp) and Kir6.2 (448 bp), and Girk2 and GAD67 fragments. All the 10 other GABAergic SNpr neurons tested showed the same expression profile for the KATP channel subunits.

molecular composition (Schwanstecher and Panten, 1993; Stanford and Lacey, 1996). The phenotype of these cells was not characterized further, but they were believed to be GABAergic. These K-ATP channels were reported to be activated by metabolic inhibition and the K channel opener diazoxide, and blocked by sulfonylureas. Our single-cell RT–mPCR analysis showed that phenotypically identified GABAergic (TH⁻, GAD67⁺, GFAP⁻) SNpr neurons presented a homogeneous pattern of K-ATP channel subunit expression ($n = 11$). In all analysed GABAergic SNpr neurons, we detected the co-expression of Kir6.2 and SUR1. SUR2 and Kir6.1 were not detected in this cell type (Figure 3C). SUR1 + Kir6.2 co-expression at the transcript level might, therefore, suggest that these subunits form the molecular basis of functional K-ATP channels in GABAergic SNpr neurons. No previous studies have addressed the question of the presence of K-ATP channels on small interneurons in the SNpc. We found no functional evidence that these GABAergic (TH⁻, GAD67⁺, GFAP⁻) interneurons in the SNpc possessed K-ATP chan-

nels. In accordance with this, in none of the analysed cells of this population ($n = 11$) could we detect the expression of K-ATP channel subunits (Figure 3B). These cells seemed, therefore, devoid of classical K-ATP channels acting as metabolic sensors. These results show that the K-ATP channel subunit expression profiles are different for two populations of GABAergic SN neurons but homogeneous within each population.

Alternative expression profiles of K-ATP channel subunits in dopaminergic SN neurons
The single-cell RT–mPCR analyis of K-ATP channel subunit expression in phenotypically defined dopaminergic SN neurons (TH⁺, GAD67⁻, GFAP⁻) revealed a heterogeneous expression pattern for the transcripts mediating the sulfonylurea receptors, SUR1 and SUR2. Three different expression pattern could be identified in the overall population of analysed dopaminergic SN neurons (Figure 4; $n = 54$). One subpopulation showed co-expression of SUR1 with Kir6.2, which represented 39% ($n = 21$ of 54) of the total population (Figure 4A). In a second major subpopulation of dopaminergic SN neurons (37%, $n = 20$ of 54), we detected the co-expression of SUR2 and Kir6.2 (Figure 4B). Finally, a third population of dopaminergic SN neurons (24%, $n = 13$ of 54) demonstrated co-expression of both SUR1 and SUR2 with Kir6.2 (Figure 4C). In accordance with the midbrain RT–PCR results, the use of SUR2 isoform-specific primer pairs showed that SUR2B but not SUR2A was expressed also at the single-cell level ($n = 5$; Figure 4D). Kir6.1 expression was not detected in dopaminergic SN neurons. These results showed that at the level of mRNA transcripts, dopaminergic in contrast to GABAergic SN neurons displayed alternative expression profiles of K-ATP channel subunits. This raised two questions. First, do dopaminergic SN neurons in contrast to GABAergic SN neurons also display a heterogeneity at the level of functional somato-dendritic K-ATP channels? Secondly, which combination(s) of K-ATP channel transcripts codes for the highly sensitive metabolic sensor in dopaminergic SN neurons and is therefore responsible for coupling metabolic stress to altered excitability?

Dopaminergic SN neurons express K-ATP channel subtypes with different sulfonylurea sensitivities
Our single-cell RT–mPCR data of dopaminergic SN neurons demonstrated a heterogeneous expression profile of K-ATP channel subunits. The alternative mRNA expression pattern of SURs in dopaminergic SN neurons predicted differences in sulfonylurea sensitivity for the level of functional K-ATP channels. Heterologous studies showed that SUR1-mediated K-ATP channels possess a higher affinity for sulfonylureas like tolbutamide compared with those containing SUR2A or SUR2B (Isomoto and Kurachi, 1997; Babenko et al., 1998; Gribble et al., 1998). To study their sulfonylurea sensitivities, neuronal K-ATP channels were activated by combining pre-incubation of the slice with 100 nM of the respiratory chain complex I blocker rotenone (>30 min) with dialysis of an ATP-free pipette solution. After 5 min of dialysis with ATP-free pipette solutions, stable current levels were obtained in all cells, although we observed differences in the washout kinetics of the K-ATP currents. Subsequently, several
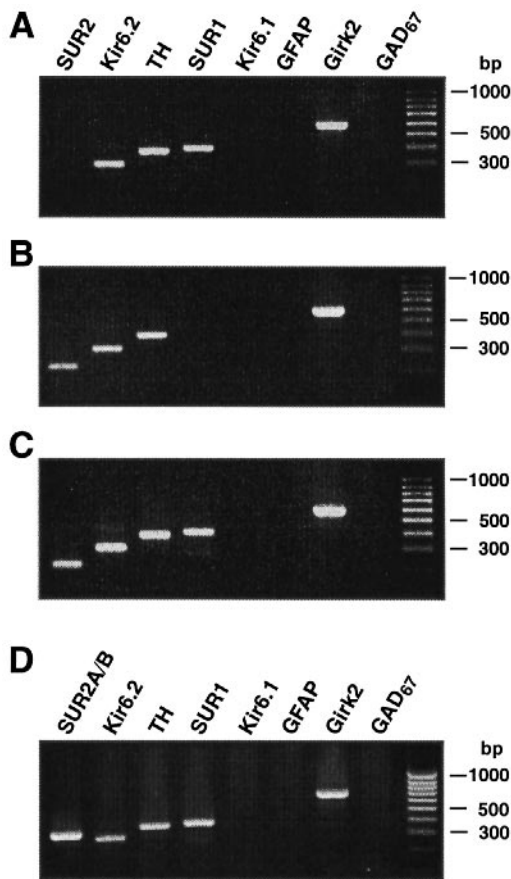
Fig. 4. Alternative SUR expression profiles in single dopaminergic SNpc neurons. mPCR expression profiling of single dopaminergic (TH$^+$, GAD67$^-$) SNpc neurons defined three dopaminergic subpopulations (A–C) with heterogeneous K-ATP subunit expression profiles. TH and Girk2 were expressed in a homogeneous fashion in all dopaminergic neurons. (**A**) Agarose gel analysis of a dopaminergic SNpc neuron of the first subpopulation where four PCR products were detected corresponding to the K-ATP channel subunits SUR1 (401 bp) and Kir6.2 (448 bp), and to the marker transcripts TH (377 bp) and Girk2 (595 bp); 21 of 54 tested neurons showed this expression profile. (**B**) Agarose gel analysis of a dopaminergic SNpc neuron of the second subpopulation where four PCR products were detected corresponding to the K-ATP channel subunits SUR2 (215 bp) and Kir6.2 (448 bp), and to the marker transcripts TH (377 bp) and Girk2 (595 bp); 20 of 54 tested neurons showed this expression profile. (**C**) Agarose gel analysis of a dopaminergic SNpc neuron of the third subpopulation where five PCR products were detected corresponding to the K-ATP channel subunits SUR1 (401 bp), SUR2 (215 bp) and Kir6.2 (448 bp), and to the marker transcripts TH (377 bp) and Girk2 (595 bp); 13 of 54 tested neurons showed this expression profile. (**D**) SUR2B is expressed in dopaminergic SNpc neurons as revealed by the use of SUR2 splice variant-specific primers in the single-cell RT–mPCR. Note that in this and four other dopaminergic neurons, only SUR2B (337 bp) but not SUR2A were detected (compare with Figure 1B).

concentrations (0.1 µM–1 mM) of the sulfonylurea tolbutamide were tested by local application via a buffer pipette. Consistent with their homogeneous SUR1 + Kir6.2 mRNA expression pattern, all GABAergic SNpr neurons displayed K-ATP channels with high sulfonylurea sensitivity. As shown in Figure 5A, the concentration dependence of tolbutamide inhibition of the whole-cell K-ATP current in GABAergic SNpr neurons was described by a Hill equation with an IC$_{50}$ value of 8.7 $\pm$ 1.7 µM and an associated Hill coefficient of 1.1 $\pm$ 0.1 (n = 8). In contrast,
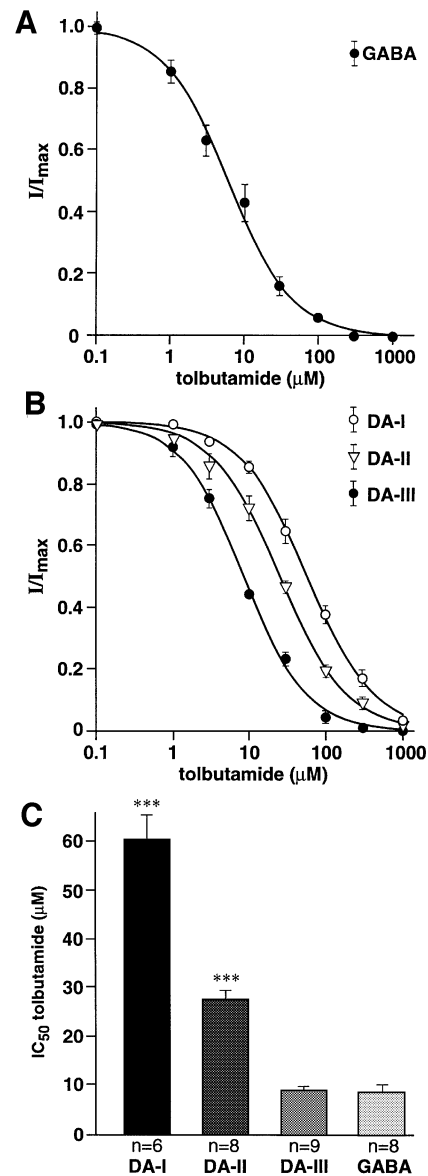

Fig. 5. K-ATP channels possess different tolbutamide sensitivities in dopaminergic SN neurons. (**A**) Concentration–response curve for tolbutamide inhibition of K-ATP whole-cell currents in GABAergic SNpr neurons activated by rotenone pre-incubation and dialysis with ATP-free pipette solutions. All points are means of eight separate experiments. Vertical lines indicate SEM; where no lines are apparent, the error was smaller than the symbol size. The line represents the fit of the mean data by a Hill equation with an IC$_{50}$ of 6.3 µM and Hill coefficient of 0.95. (**B**) Concentration–response curves for tolbutamide inhibition of K-ATP whole-cell currents in dopaminergic SN neurons activated by rotenone pre-incubation and dialysis with ATP-free pipette solutions. All points are means of 6–9 separate experiments. Vertical lines indicate SEM; where no lines are apparent, the error was smaller than the symbol size. The lines represent the fits of the mean data of three different subpopulations (DA-I, DA-II and DA-III) by Hill equations (DA-I: IC$_{50}$ = 58 µM, Hill coefficient = 0.98; DA-II: IC$_{50}$ = 25.0 µM, Hill coefficient = 0.95; DA-III: IC$_{50}$ = 8.5 µM, Hill coefficient = 1.08). (**C**) The mean IC$_{50}$s for the tolbutamide sensitivity of K-ATP whole-cell currents in GABAergic SNpr and dopaminergic SN neurons. Data were obtained by fitting Hill equations to the tolbutamide concentration–response curves determined for individual GABAergic and dopaminergic SN neurons. Error bars indicate SEM and n shows the number of neurons in each group. The asterisks indicate significant differences (t-test; p <0.0001) in tolbutamide sensitivity for DA-I and DA-II compared with DA-III and GABA.

dopaminergic SN neurons ($n = 23$) displayed different sensitivities to tolbutamide inhibition (Figure 5B). A total of 40% (nine of 23) of the cells possessed a high affinity for tolbutamide which was described by a Hill equation with an IC_{50} value of 8.8 ± 1.0 µM and a Hill coefficient of 1.2 ± 0.1. K-ATP channels in a second group ($n = 6$) of dopaminergic SN neurons showed a 7-fold lower sulfonylurea sensitivity ($IC_{50} = 60.6 ± 5.1$ µM; Hill coefficient = 1.0 ± 0.1, $n = 6$). In a third population of dopaminergic SN neurons ($n = 8$), functional K-ATP channels were activated which possessed an intermediate sulfonylurea sensitivity, with an IC_{50} of 27.9 ± 1.9 µM and a Hill coefficient of 1.1 ± 0.1. For these cells, the concentration dependence of tolbutamide inhibition was not well described by the sum of two Hill equations with a high and low IC_{50} value but rather with a single Hill equation with an intermediate sulfonylurea sensitivity. The tolbutamide sensitivities of the three populations of dopaminergic SN neurons were significantly different ($p > 0.0005$) and those with the highest sensitivity were similar to that of the GABAergic SNpr neurons (Figure 5C). In accordance with our single-cell RT–mPCR data, these pharmacological results demonstrated that GABAergic SNpr neurons possess a homogeneous population of K-ATP channels with a high SUR1-like sulfonylurea sensitivity. In contrast, dopaminergic SN neurons functionally express multiple K-ATP channel species distinguished by different affinities for sulfonylureas.

K-ATP channel subtypes in dopaminergic SN neurons display large differences in metabolic sensitivities

The results presented so far indicate that dopaminergic SN neurons express molecularly and pharmacologically distinct K-ATP channels. Our main interest was to ask whether these K-ATP channel types also possess functionally relevant differences. One of the most important differences between alternative K-ATP channel types would concern their metabolic sensitivity. Major differences in the metabolic sensitivity of K-ATP channels in dopaminergic SN neurons were apparent from two sets of experiments: either when the slices were pre-incubated with nanomolar concentrations of the complex I inhibitor rotenone or when 10 µM rotenone was applied locally to a patch-clamped neuron. In acute experiments, application of 10 µM rotenone led to activation of a K conductance which was voltage and time independent and showed little to no rectification in the subthreshold voltage range between –120 and –40 mV in a subpopulation of dopaminergic SN neurons. Current-clamp recordings showed that rotenone induced a mean hyperpolarization to –60.9 ± 1.9 mV from resting potentials in the range of –40 to –45 mV ($n = 14$). The hyperpolarization was accompanied by a complete cessation of spontaneous electrical activity and was inhibited by 100 µM tolbutamide (Figure 6A). Co-application of glibenclamide (100 nM, $n = 38$; Figure 6C) or tolbutamide (100 µM, $n = 5$; Figure 6B) completely blocked the induced K conductance, and the current amplitudes returned to control levels. Whereas the block by tolbutamide was readily reversible, inhibition by glibenclamide was irreversible even after prolonged periods (>40 min) of washout. These experiments demonstrated that complex I inhibition selectively activated

K-ATP channels with a sulfonylurea sensitivity which corresponded to the most sensitive subtype defined by the pharmacological experiments (Figure 5B). Voltage ramps showed that the K-ATP whole-cell conductances induced by complex I inhibition (2.2 ± 0.2 nS, $n = 12$) reversed close to E_K (104.0 ± 1.1 mV, $n = 12$; Figure 6B). We also identified a subpopulation (37%, $n = 25$ of 68) of dopaminergic SN neurons which showed no detectable change in membrane conductance during acute application of 10 µM rotenone (Figure 6D). Application of 10 µM rotenone to neurons which were dialysed with a pipette solution containing 2 mM ATP in the standard whole-cell configuration was not sufficient to activate the other K-ATP channel species with lower sulfonylurea sensitivities. It is likely that the standard whole-cell configuration *per se* will alter the metabolic threshold for K-ATP channel activation by washout of activating metabolites and the coupling of the cell to a virtually unlimited pool of ATP via the patch pipette.

To overcome these limitations, we investigated the threshold for K-ATP channel activation by complex I inhibition in metabolically intact cells by pre-incubation of the slice for >30 min in rotenone concentrations ranging from 1 nM to 10 µM. A 10 µM concentration of rotenone was the upper limit because pre-incubation with higher concentrations induced a fast disintegration of the midbrain slice. After the pre-incubation period, K-ATP currents and membrane potential of dopaminergic SN neurons were analysed immediately after obtaining the standard whole-cell configuration to minimize secondary washout effects. This second type of metabolic experiment confirmed that dopaminergic SN neurons indeed possess different thresholds for K-ATP channel activation. In one group of neurons, K-ATP channel activation and membrane hyperpolarization accompanied by loss of spontaneous activity were already observed in the presence of low nanomolar concentrations of rotenone. In 100 nM rotenone, these neurons showed large K-ATP currents and membrane hyperpolarizations greater than –65 mV (Figure 7A, $n = 8$). In addition, K-ATP channels were fully activated because dialysis with ATP-free pipette solutions did not enhance further the outward currents that were observed immediately after establishing the whole-cell configuration (Figure 7A). The mean rotenone concentration dependence of membrane hyperpolarization for this dopaminergic subpopulation was described by a Hill equation with an EC_{50} of 14.5 nM, a Hill coefficient of 0.78 and a maximal membrane hyperpolarization to –68.1 mV (Figure 7B, $n = 6–10$). The mean rotenone concentration dependence of activation of this K-ATP channel subpopulation was described by a Hill equation with an EC_{50} of 16.2 nM, a Hill coefficient of 0.94 and a maximal K-ATP conductance of 7.1 nS (Figure 7C, $n = 6–10$). Co-pre-incubation of the slice with 100 nM rotenone and 100 µM tolbutamide completely prevented the activation of K-ATP channels in all dopaminergic SN neurons (subthreshold slope conductance: control: 1.5 ± 0.1 nS, $n = 12$; 100 nM rotenone: 7.7 ± 0.9 nS, $n = 8$; 100 nM rotenone + 100 µM tolbutamide: 1.6 ± 0.1 nS, $n = 10$).

A second population of dopaminergic SN neurons was not affected by pre-incubation of nanomolar concentrations of rotenone, and K-ATP channels were only partially
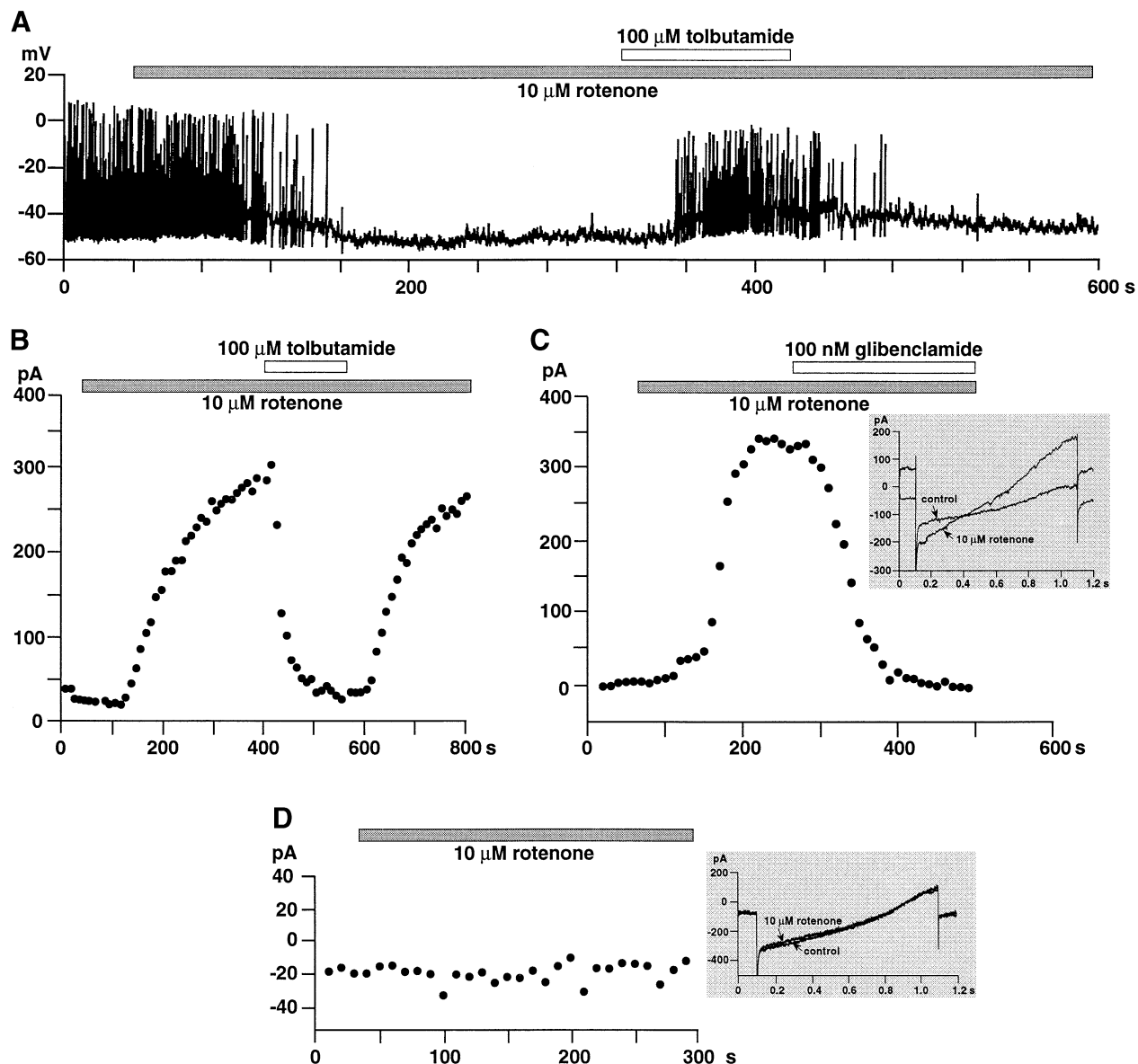
Fig. 6. Activation of K-ATP channels with high sulfonylurea affinity in a subpopulation of dopaminergic SN neurons by local application of 10 μM rotenone. (**A**) Current-clamp recording of a dopaminergic SN neuron. Application of 10 μM rotenone (indicated by the bar) led to hyperpolarization and complete cessation of spontaneous pacemaker activity which was completely reversed by the co-application of 100 μM tolbutamide. (B–D) Current responses evoked by 10 mV depolarizing voltage steps from a holding potential of –60 mV of voltage-clamped dopaminergic SNpc neurons (drug applications indicated by bars). (**B**) Application of 10 μM rotenone activated outward K currents which were completely and reversibly blocked by co-application of 100 μM tolbutamide. (**C**) Rotenone-activated K currents were completely blocked by 100 nM glibenclamide (insert: current responses to voltage ramps from –120 to –40 mV before and during application of rotenone showed that the rotenone-evoked current reversed close to E_K). Forty-three of 68 dopamineric SN neurons showed K-ATP currents activated by acute application of rotenone. (**D**) A subpopulation of dopaminergic SN neurons did not respond to local rotenone application. This and another 24 of 68 tested dopaminergic SNpc neurons showed no current activation by acute application of 10 μM rotenone (insert: current responses to voltage ramps from –120 to –40 mV before and during application of rotenone).

activated by rotenone concentrations of 1–10 μM. In 100 nM rotenone, these neurons presented subthreshold slope conductances and pacemaker activity similar to those observed under metabolic control conditions (Figure 7D). K-ATP channels were closed in the presence of 100 nM rotenone and only activated by dialysis with ATP-free pipette solutions (Figure 7D). The mean rotenone concentration dependence of membrane hyper-polarization for this dopaminergic subpopulation was described by a Hill equation with an EC_{50} of 1.2 μM, a Hill coefficient of 1 and a maximal membrane hyperpolar-

ization to –58.3 mV (Figure 7E, $n = 6$–10). The mean rotenone concentration dependence of K-ATP channel activation in this population was described by a Hill equation with an EC_{50} of 3.6 μM (Hill coefficient = 1.0, maximum K-ATP conductance = 3.9 nS), corresponding to >200-fold lower metabolic sensitivity compared with the K-ATP channels activated in the nanomolar range (Figure 7F). Co-pre-incubation of 10 μM rotenone with 100 μM tolbutamide only partially prevented the activation of K-ATP channels in this subpopulation (subthreshold slope conductance: 10 μM rotenone: 4.5 ± 0.2 nS, $n =$
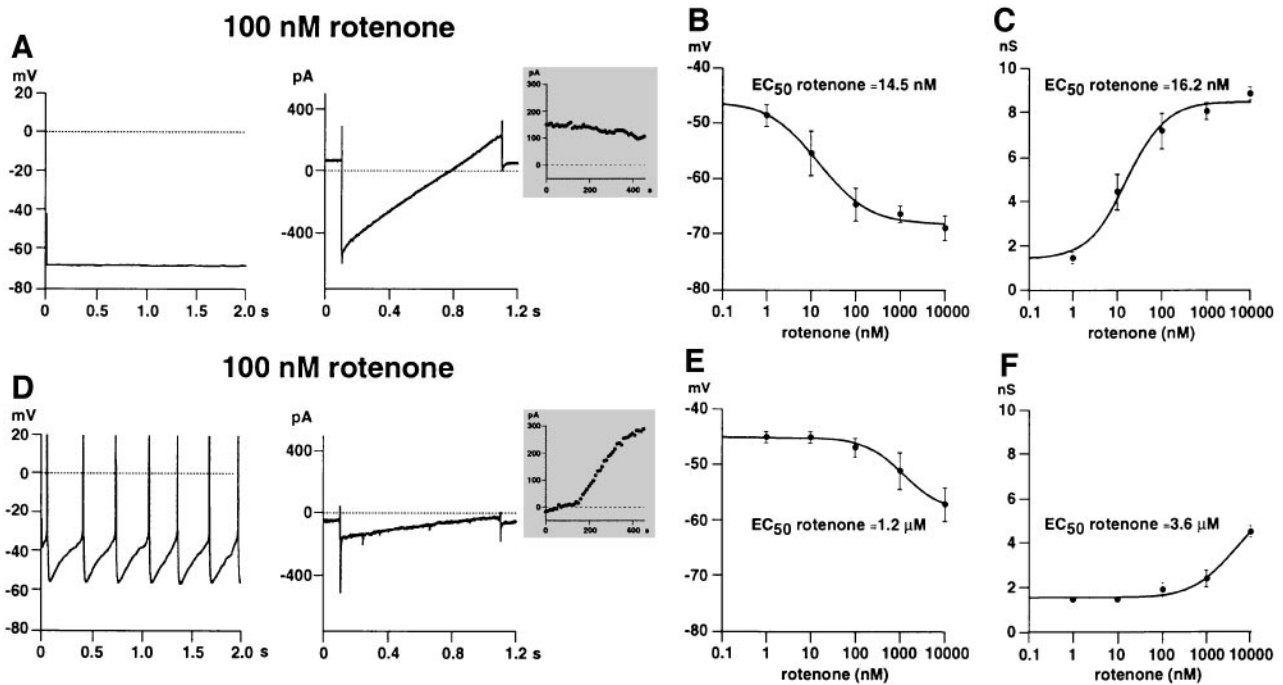
Fig. 7. Rotenone pre-incubation reveals K-ATP channels with different metabolic sensitivities in dopaminergic SN neurons. (**A**) Properties of dopaminergic SN neurons sensitive to pre-incubation with 100 nM rotenone. Membrane potential in current-clamp (left panel) and current response to a voltage ramp (–120 to –40 mV from a holding potential of –60 mV; middle panel). Recordings were performed immediately after obtaining the standard whole-cell configuration. The right panel plots the current responses evoked by 10 mV depolarizing voltage steps from a holding potential of –60 mV in a dopaminergic SN neuron dialysed with ATP-free pipette solution. Note that the K-ATP whole-cell current was activated fully immediately after establishing the whole-cell configuration, and no further ATP washout current developed with time. (**B**) Rotenone concentration dependence of membrane hyperpolarization in dopaminergic SN neurons with high metabolic sensitivity. All points are means of 6–10 separate experiments. Here, and in (C), (E) and (F), the vertical lines indicate SEM; where no lines are apparent, the error was smaller than the symbol size. The line represents the fit of the mean data by a Hill equation with an EC_{50} of 14.5 nM and Hill coefficient of 0.78. The fitted control membrane potential was –46.0 mV and the maximal rotenone-induced hyperpolarization was –68.1 mV. (**C**) Rotenone concentration dependence of K-ATP channel activation with high metabolic sensitivity in dopaminergic SN neurons. All points are means of 6–10 separate experiments. The line represents the fit of the mean data by a Hill equation with an EC_{50} of 16.2 nM and Hill coefficient of 0.94. The fitted control conductance was 1.4 nS and the maximal K-ATP conductance was 7.12 nS. (**D**) Properties of dopaminergic SN neurons insensitive to pre-incubation with 100 nM rotenone. Membrane potential in current-clamp (left panel) and current response to a voltage ramp (–120 to –40 mV from a holding potential of –60 mV; middle panel). Recordings were performed immediately after obtaining the standard whole-cell configuration. The right panel plots the current responses evoked by 10 mV depolarizing voltage steps from a holding potential of –60 mV in a dopaminergic SN neuron dialysed with ATP-free pipette solution. Note that no K-ATP whole-cell current was apparent immediately after establishing the whole-cell configuration but was activated by ATP washout. (**E**) Rotenone concentration dependence of membrane hyperpolarization in dopaminergic SN neurons with low metabolic sensitivity. All points are means of 6–10 separate experiments. The line represents the fit of the mean data by a Hill equation with an EC_{50} of 1.2 μM, a Hill coefficient of 1 and a maximal hyperpolarization to –58.3 mV. (**F**) Rotenone concentration dependence of K-ATP channel activation with low metabolic sensitivity in dopaminergic SN neurons. All points are means of 6–10 separate experiments. The line represents the fit of the mean data by a Hill equation with an EC_{50} of 3.6 μM and Hill coefficient of 1.0. The fitted control conductance was 1.56 nS and the maximal K-ATP conductance 3.9 nS.

8; 10 μM rotenone + 100 μM tolbutamide: 2.8 ± 0.2 nS, $n = 8$). The partial block of K-ATP channels with low metabolic sensitivity by 100 μM tolbutamide indicated that they correspond to those with low sulfonylurea affinity (IC_{50} tolbutamide = 60 μM; Figure 5B).

Like complex I inhibition, pre-incubation of the slice for >30 min in iodoacetate, an inhibitor of glycolysis in concentrations ranging from 1 to 300 μM, also activated two types of K-ATP channels with high (EC_{50} = 17 μM, Hill coefficient = 2.5, maximum K-ATP conductance = 5.6 nS, $n = 4$–6) and low (EC_{50} = 1.2 mM, Hill coefficient = 1, maximum K-ATP conductance = 5.5 nS, $n = 4$–6) metabolic sensitivities. Again, only K-ATP channels with high affinity for iodoacetate were blocked completely by co-pre-incubation with 100 μM tolbutamide (subthreshold slope conductance: control: 1.4 ± 0.1 nS, $n = 6$; 100 μM iodoacetate: 7.2 ± 0.6 nS, $n = 6$; 100 μM iodoacetate + 100 μM tolbutamide: 1.5 ± 0.2 nS, $n =$

7). In summary, these experiments clearly indicated that dopaminergic SN neurons possess at least two functionally different types of K-ATP channels with large differences in their sensitivities to metabolic inhibition (>200-fold for complex I inhibition; >70-fold for inhibition of glycolysis).

Differential sensitivity to metabolic inhibition correlates with alternative SUR mRNA expression at the level of single dopaminergic SN neurons

To test directly the hypothesis that alternative SUR expression is correlated with differential metabolic sensitivity, we combined rotenone pre-incubation with our single-cell RT–mPCR protocol. After pre-incubation with 100 nM rotenone, membrane potentials and subthreshold conductances were analysed immediately after obtaining the whole-cell configuration. Subsequently, the cytoplasm of the cells was harvested and used for single-cell RT–
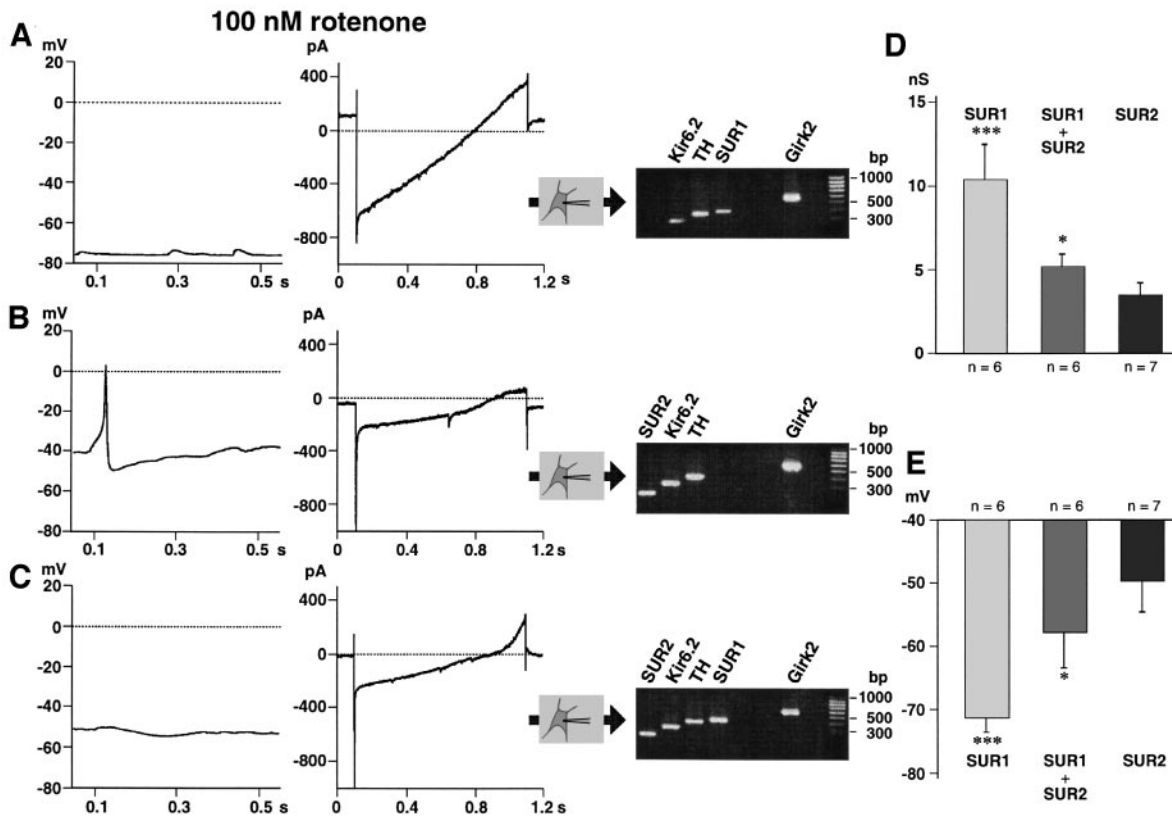
Fig. 8. Alternative SUR expression correlates with different metabolic sensitivities of K-ATP channels in single dopaminergic SN neurons. (A–C) Properties of dopaminergic SN neurons after pre-incubation with 100 nM rotenone. Membrane potentials in current-clamp (left panel) and current responses to a voltage-ramp (–120 to –40 mV from a holding potential of –60 mV; middle panel). Recordings were performed immediately after obtaining the standard whole-cell configuration. After electrophysiological characterization, the cytoplasm of cells was harvested for single-cell RT–mPCR analysis. Agarose gel analysis-displayed expression profile of K-ATP-channel subunits: (**A**) SUR1 (401 bp) + Kir6.2 (448 bp); (**B**) SUR2 (215 bp) + Kir6.2; and (**C**) SUR1 + SUR2 + Kir6.2 in combination with markers TH (377 bp) and Girk2 (595 bp). (**D**) Mean subthreshold conductances induced by rotenone pre-incubation (100 nM) of dopaminergic SN subpopulations defined by alternative SUR expression. Errors are given as SEM, and n shows the number of neurons in each group. Asterisks indicate statistically significant differences between the subgroups (t-test: SUR1 versus SUR2, $p < 0.0005$; SUR1 versus SUR1 + SUR2, $p < 0.05$; SUR1 + SUR2 versus SUR2, $p < 0.05$). (**E**) Mean membrane hyperpolarization induced by rotenone pre-incubation (100 nM) of dopaminergic SN subpopulations defined by alternative SUR expression. Errors are given as SEM, and n shows the number of neurons in each group. Asterisks indicate statistically significant differences between the subgroups (t-test: SUR1 versus SUR2, $p < 0.0005$; SUR1 versus SUR1 + SUR2, $p < 0.05$; SUR1 + SUR2 versus SUR2, $p < 0.05$).

mPCR. Dopaminergic SN neurons which showed the highest sensitivity for metabolic inhibition, evident by a large K-ATP whole-cell conductance and strong membrane hyperpolarization, expressed the K-ATP channel subunit combination SUR1 + Kir6.2 (Figure 8A). This is consistent with our finding that K-ATP channels with the highest metabolic sensitivity were also characterized by a high affinity for sulfonylureas. In contrast, for cells that were unresponsive to pre-incubation with 100 nM rotenone, co-expression of SUR2B + Kir6.2 was determined (Figure 8B). An intermediate response with a smaller hyperpolarization to about –55 mV and increases of subthreshold conductances to ~5 nS was found for cells co-expressing both sulfonylurea receptors SUR1 + SUR2B with Kir6.2 (Figure 8C). Under metabolic control conditions, no electrophysiological differences were apparent between neurons with alternative SUR expression pattern (subthreshold slope conductance: SUR1: 1.5 ± 0.1 nS, $n = 12$; SUR2B: 1.4 ± 0.2 nS, $n = 7$; SUR1 + SUR2B: 1.5 ± 0.3 nS, $n = 4$). The data for the 19 cells studied in this combined metabolic–molecular experiment are summarzied in Figure 8D and E. They demonstrate

that the alternative co-expression of sulfonylurea receptors in dopaminergic SN neurons is correlated with highly significant differences (SUR1 versus SUR2: $p < 0.0005$) in the functional response to inhibition of mitochondrial metabolism.

Surviving dopaminergic SN neurons in the weaver mouse exclusively express SUR1-mediated K-ATP channels

To test whether a particular SUR expression profile is correlated with the surviving population of dopaminergic SN neurons, we analysed their K-ATP channel expression profiles in 14-day-old homozygous *weaver* mice. The *weaver* mouse is a genetic model of selective degeneration of a subpopulation of highly vulnerable dopaminergic midbrain neurons caused by a pore mutation in a G-protein-activated inwardly rectifying K channel (Girk2) (Patil *et al.*, 1995). All analysed dopaminergic SN neurons in homozygous *weaver* (*wv/wv*) mouse exclusively expressed SUR1 + Kir 6.2 (Figure 9A; $n = 22$). In contrast, dopaminergic SN neurons of unaffected littermates (+/+) displayed a similar distribution of the
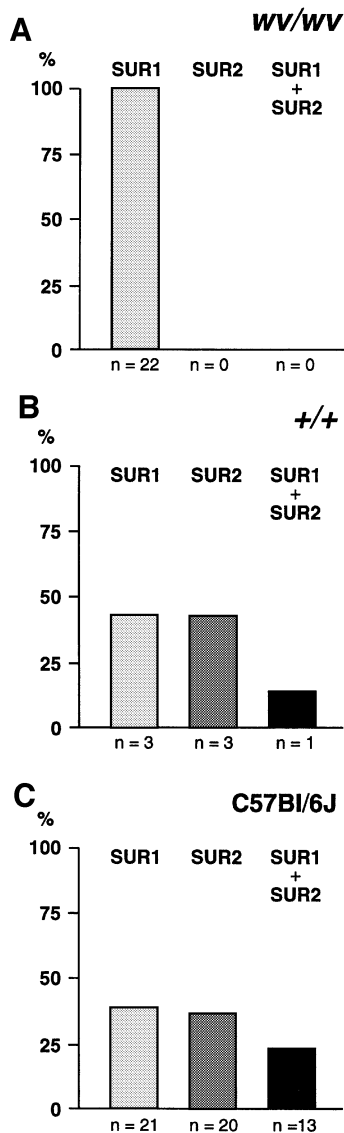
Fig. 9. Homogeneous SUR1 expression in surviving dopaminergic SN neurons of a homozygous *weaver* mouse. Distribution of SUR isoform expression in dopaminergic (TH$^+$) SN neurons from (**A**) homozygous *weaver* (*wv/wv*) mice ($n = 22$), (**B**) homozygous normal (+/+) controls ($n = 7$) and (**C**) C57Bl/6J mice ($n = 54$). Note the absence of SUR2 expression in *wv/wv* dopaminergic SN neurons and the similiar SUR isoform distribution in dopaminergic SN neurons from C57Bl/6J and (+/+) B6/CBA-A^{w-j}/AC mice.

alternative SUR isoform expression as those from C57Bl/6J mice (Figure 9B and C). These SUR1-containing K-ATP channels were already partially activated under metabolic control conditions in *wv/wv* dopaminergic SN neurons and were completely blocked by 100 μM tolbutamide (*wv/wv* K-ATP conductance: 1.2 ± 0.3 nS, $n = 9$). These results suggest that alternative SUR expression is relevant in the context of neurodegeneration and that expression of SUR1-containing K-ATP channels might play a protective role for dopaminergic SN neurons during the active period of neurodegeneration in the *weaver* mouse.

Discussion

Expression profiling of K-ATP subunits in phenotypically identified single midbrain neurons by RT–mPCR

In the present study, we have determined the mRNA expression profiles of K-ATP channel subunits in three populations of wild-type and *weaver* mouse midbrain neurons at the level of single neurons using an RT–mPCR approach ($n = 128$). The sensitivity of the single-cell RT–mPCR protocol which combined two rounds of PCR (multiplex + nested) was optimized using highly diluted mouse midbrain cDNA to obtain an estimated subfemto-molar detection threshold suitable for single-cell transcripts. The neurons were characterized phenotypically by co-amplification of a panel of marker transcripts (TH, GAD67 and GFAP) in order to differentiate between dopaminergic and GABAergic neurons, and to exclude astroglial cells. Identified dopaminergic (TH$^+$) SN neurons uniformly displayed their previously described typical electrophysiological properties, i.e. slow spontaneous pacemaker activity, broad action potentials with depolarized thresholds and a strong I_h component (Grace and Onn, 1989; Lacey *et al.*, 1989; Condé, 1992; Richards *et al.*, 1997). The small GAD67$^+$ neurons within the SNpc most likely correspond to the previously reported SNpc type II neurons which displayed faster spontaneous activity and possessed no I_h or subthreshold A current (Lacey *et al.*, 1989; Johnson and North, 1992). The larger GAD67$^+$ neurons recorded in the SNpr showed similar properties to GABAergic projection neurons studied in rat brain slices (Stanford and Lacey, 1996; Richards *et al.*, 1997).

Our single-cell RT–mPCR protocol probed for the mRNA expression of the cloned subunits currently thought to be involved in the formation of different K-ATP channels (Bryan and Aguilar-Bryan, 1997; Quale *et al.*, 1997; Yokoshiki *et al.*, 1998). GABAergic neurons of the SNpr showed a homogeneous K-ATP channel subunit profile, with SUR1 and Kir6.2 co-expression detected in all cells. This subunit combination leads to β-cell-like K-ATP channels in heterologous expression systems (Inagaki *et al.*, 1995a; Gribble *et al.*, 1997). SUR1 + Kir6.2-mediated K-ATP channels are activated by diazoxide and metabolic inhibition, and are blocked with high affinity by sulfonylureas such as glibenclamide and tolbutamide. In accordance with our single-cell RT–mPCR data, all GABAergic SNpr neurons expressed K-ATP channels with high tolbutamide sensitivity (IC$_{50}$ = 8.7 μM). Our results are in agreement with other electrophysiological studies demonstrating SUR1-like K-ATP channels on SNpr neurons (Schwanstecher and Panten, 1993; Stanford and Lacey, 1996). In contrast, GABAergic interneurons in the SNpc did not express any of the K-ATP channel subunits. In these cells, we could, in contrast, detect the presence of Girk2 transcripts, indicating that the amount of harvested material was sufficient to detect low abundance ion channel mRNA. As we also did not observe functional K-ATP channels in these neurons, our results suggest that GABAergic SNpc interneurons do not express SUR1- or SUR2B-mediated K-ATP channels.

Molecular and pharmacological diversity of K-ATP channels in dopaminergic SN neurons

In contrast to the homogeneous K-ATP subunit expression profiles detected in GABAergic SN neurons, the pattern

of K-ATP subunit expression was more complex for dopaminergic SN neurons. We defined three populations with alternative K-ATP subunit expression profiles. In the two major populations, the transcripts for the pore-forming part of the K-ATP channel, Kir6.2, was co-expressed with the mRNA for either SUR1 (39%) or SUR2B (37%). The remaining population displayed co-expression of both SUR1 and SUR2B with Kir6.2 (24%). In correspondence with the single-cell RT–mPCR results, we observed functional K-ATP channels with significant differences in sulfonylurea sensitivities in dopaminergic SN neurons. The K-ATP channel population with the highest tolbutamide sensitivity (IC_{50} = 8.8 μM) was indistinguishable from that found in GABAergic SNpr neurons. This K-ATP channel subtype is therefore likely to be mediated by SUR1 + Kir6.2 co-expression. In heterologous expression systems, SUR2-mediated K-ATP channels show a lower sulfonylurea sensitivity compared with SUR1-mediated channels (Isomoto and Kurachi, 1997; Babenko et al., 1998; Gribble et al., 1998). Thus, it is reasonable to assume that the K-ATP channels with the lowest tolbutamide sensitivity (IC_{50} = 60.6 μM) are formed by SUR2B + Kir6.2 co-expression in dopaminergic SN neurons. It is unknown whether SUR1 and SUR2B form functional heterooligomeric K-ATP channels in the presence of Kir6.2. However, both our single-cell RT–mPCR results demonstrating SUR1 + SUR2B co-expression in single neurons and the identification of K-ATP channels with intermediate sulfonylurea sensitivity (IC_{50} = 27.9 μM) suggest this possibility.

Our analysis demonstrated the diversity of K-ATP subunit expression profiles in midbrain neurons. Two recent reports analysing the K-ATP subunit expression in three rat dorsal vagal neurons (SUR1 + Kir6.2) and five rat striatal interneurons (SUR1 + Kir6.1) further illustrate the molecular complexity of neural K-ATP channels (Karschin et al., 1998; Lee et al., 1998).

Alternative sulfonylurea receptor expression correlates with metabolic sensitivity of K-ATP channels in single dopaminergic SN neurons

Our results show that K-ATP channels with very large differences in metabolic sensitivity (70- to 200-fold) were activated in dopaminergic SN neurons by inhibition of both mitochondrial complex I and glycolysis. K-ATP channels which were highly responsive to metabolic inhibition were completely blocked by 100 μM tolbutamide, indicating that they possess a high affinity for sulfonylureas, while low sensitivity K-ATP channels were only partially blocked by this concentration of tolbutamide. Although sulfonylurea sensitivity of K-ATP channels might be modulated by other factors in addition to subunit composition (Brady et al., 1998), the correlation between expression profiles and pharmacological properties demonstrated for GABAergic and dopaminergic SN neurons in this study suggested that SUR1 is involved in the formation of K-ATP channels acting as highly sensitive metabolic response elements. We tested this hypothesis directly by combining rotenone pre-incubation with the single-cell RT–mPCR protocol. Our results clearly demonstrate, at the level of individual neurons, that cells with fully activated K-ATP channels and large membrane hyperpolarizations in response to 100 nM rotenone co-express SUR1

+ Kir6.2, while unresponsive cells co-expressed SUR2B + Kir6.2. The neurons which possessed both SUR1 and SUR2B at the transcript level showed an intermediate metabolic sensitivity. Although the molecular mechanisms remain undefined, a higher metabolic sensitivity has also been reported for heterologously expressed SUR1-containing channels compared with SUR2-containing channels (Ashcroft and Gribble, 1998), indicating that differences in metabolic sensing might indeed be linked directly to alternative expression of SUR isoforms. Much has been speculated about the functional response of dopaminergic SN neurons to partial inhibition of mitochondrial complex I activity which is present in Parkinson's disease (Hanna and Bhatia, 1997). The selective activation of SUR1-containing K-ATP channels by low nanomolar concentrations of rotenone, which corresponds to a partial complex I inhibition, identifies this K-ATP channel subtype as a sensitive target for the metabolic challenge of Parkinson's disease.

K-ATP channel expression in surviving dopaminergic SN neurons of weaver mouse: alternative SUR expression as a candidate mechanism for differential vulnerability in neurodegeneration?

In striking contrast to the alternative SUR expression profiles detected in dopaminergic SN neurons of wild-type mice [C57Bl/6J and (+/+) B6/CBA-A$^{w–j}$/AC], all analysed neurons in homozygous weaver (wv/wv) mice exclusively expressed SUR1 + Kir6.2. In addition, these SUR1-containing K-ATP channels were already partially activated under metabolic control conditions in wv/wv dopaminergic SN neurons. The weaver mouse is a genetic model for the selective degeneration of a highly vulnerable subpopulation of dopaminergic SN neurons (Bayer et al., 1995; Patil et al., 1995). At postnatal day 14, which is the age we investigated, 35% of dopaminergic SN neurons are already lost (Verney et al., 1995). Our findings that SUR2 expression was never detected in surviving dopaminergic wv/wv neurons and that 37% of wild-type dopaminergic SN neurons express only SUR2 might indicate that the SUR2-expressing subpopulation of dopaminergic SN neurons corresponds to that possessing high vulnerability. Furthermore, all surviving dopaminergic wv/wv neurons exclusively expressed SUR1. This suggests that the activity of SUR1-containing K-ATP channels might have a neuroprotective role in the weaver mouse. There are great similarites in the pattern of differential vulnerability of dopaminergic subpopulations between the weaver mouse and Parkinson's disease (Gaspar et al., 1994). Thus, it is conceivable that alternative SUR expression also constitues a molecular mechanism involved in the differential vulnerability of dopaminergic neurons in Parkinson's disease.

Materials and methods

Slice preparation
Young C57Bl/6J (12–16 days old), unaffected (+/+) and homozygous (wv/wv) weaver (B6/CBA-A$^{w–j}$/AC; 14 days old) mice were anaesthetized deeply with halothane and then decapitated. Weaver mice were genotyped by genomic DNA sequencing. Brains were removed quickly, immersed in ice-cold solution, and then blocked for slicing. Thin coronal midbrain slices (200–250 μm) were cut with a Vibroslice (Campden Instruments,

London, UK) while bathed in an ice-cold artificial cerebrospinal fluid (ACSF) containing: 125 mM NaCl, 25 mM NaHCO$_3$, 2.5 mM KCl, 1.25 mM NaH$_2$PO$_4$, 2 mM CaCl$_2$, 2 mM MgCl$_2$ and 25 mM glucose, bubbled with a mixture of 95% O$_2$/5% CO$_2$. After sectioning, midbrain slices were maintained submerged in a holding chamber filled with gassed ACSF, and allowed to recover for >30 min at room temperature (22–24°C) before the experiment. The midbrain slices containing a clearly defined substantia nigra pars compacta at the level of the rostral interpeduncularis nucleus and the caudal mammillary nucleus (corresponding to levels 2 and 3; Nelson *et al.*, 1996) were used for the experiments.

Whole-cell recordings and data analysis

For patch-clamp recordings, midbrain slices were transferred to a chamber continuously perfused at 2–4 ml/min with ACSF bubbled with a mixture of 95% O$_2$/5% CO$_2$ at room temperature (22–24°C). Patch pipettes (1–2.5 MΩ) pulled from borosilicate glass (GC150TF, Clark, Reading, UK) were filled with internal solution containing: 120 mM K-gluconate, 20 mM KCl, 10 mM HEPES, 10 mM EGTA, 2 mM MgCl$_2$, 2 mM Na$_2$ATP, pH 7.3 (290–300 mOsm). Whole-cell recordings were made from substantia nigra neurons visualized by infrared differential interference contrast (IR-DIC) videomicroscopy with a Newvicon camera (C2400, Hamamatsu, Hamamatsu City, Japan) mounted on an upright microscope (Axioskop FS, Zeiss, Oberkochen, Germany) (Stuart *et al.*, 1993). Recordings were carried out in current-clamp and voltage-clamp mode using an EPC-9 patch-clamp amplifier (HEKA Elektronik, Lambrecht, Germany). Only experiments with uncompensated series resistances <10 MΩ were included in the study, and series resistances were compensated electronically (50–75%). The program package PULSE+PULSEFIT (HEKA Elektronik, Lambrecht, Germany) was used for data acquisition and analysis. Leakage and capacitive currents were subtracted on-line using the P/4 subtraction method as indicated. Records were digitized at 2–5 kHz and filtered with a low-pass filter Bessel characteristic of a 1 kHz cut-off frequency. Dimethylsulfoxide (DMSO) or NaOH stock solutions of the drugs were diluted 1000-fold in an external solution containing: 145 mM NaCl, 2.5 mM KCl, 10 mM HEPES, 2 mM CaCl$_2$, 2 mM MgCl$_2$ and 25 mM glucose (pH 7.4) and applied locally under visual control using a macro-patch pipette attached to a second manipulator. Switching between control and drug-containing solutions was controlled by an automated application system (Automate, USA). For pre-incubation experiments, drugs were added to ACSF. Concentration–response data were fitted according to the relationships for tolbutamide inhibiton, $I/I_{max} = 1/(1 + ([tolbutamide]/IC_{50})^n)$; rotenone-induced activation (nS), $f1 = a*(1 - 1/(1 + ([rotenone]/IC_{50})^n) + b$; rotenone-induced hyperpolarization (mV), $f2 = -c*(1 - 1/(1 + ([rotenone]/IC_{50})^n) + d$. f1 corresponds to membrane conductance (nS), f2 = membrane potential (mV), IC_{50} = half-maximal concentration, n = Hill coefficient, a = maximal conductance induced by rotenone, b = control conductance, c = maximal hyperpolarization induced by rotenone and d = control membrane potential. To evaluate statistical significance, data were subjected to Student's *t*-test in SIGMAPLOT (Jandel).

Cytoplasm harvest and reverse transcription

For single-cell RT–PCR experiments, the patch pipettes were filled with 6 µl of autoclaved internal RT–PCR solution containing: 140 mM KCl, 5 mM HEPES, 5 mM EGTA, 3 mM MgCl$_2$, pH 7.3. At the end of the recording (<15 min), the cell contents (including the nucleus, in most cases) were aspirated as completely as possible into the patch pipette under visual control (40× objective + 2–4× zoom) by application of gentle negative pressure. Cells were only analysed further when the whole-cell configuration remained stable throughout the harvesting proceedure. Pipettes were then quickly removed from the cell, washed twice through the solution interface, and the pipette contents were expelled immediately into a 0.5 ml test tube containing the contents for reverse transcription. First strand cDNA was synthesized for 1 h at 37°C in a total reaction volume of 10 µl containing random hexamer primers (Boehringer Mannheim, final concentration 5 µM), dithiothreitol (final concentration 10 mM), the four deoxyribonucleotide triphosphates (Pharmacia, final concentration 0.5 mM each), 20 U of ribonuclease inhibitor (Promega) and 100 U of reverse transcriptase (Superscript™II; Gibco-BRL). The single-cell cDNA was kept at –70°C until PCR amplification.

Multiplex and nested PCR

Following reverse transcription, the cDNAs for Kir6.2, Kir6.1, SUR1, SUR2 (alternatively SUR2A and SUR2B), TH, Girk2, GFAP and GAD67 were amplified simultaneously in a multiplex PCR using the following

set of primers (from 5′ to 3′): Kir6.2 (accession No. D50581) sense, AAGAAAGGCAACTGCAACGT (position 243), antisense, CCCCAT-AGAATCTCGTCAGC (position 1066); Kir6.1 (accession No. D88159) sense, GTCTTCTAGGAGGACGCGTG (position 126), antisense, TAT-CATACAGGGGGCTACGC (position 786); SUR1 (accesssion No. for rat sequence L40624) sense, GTGAGTTCCTGTCCAGTGCA (position rat 2091), antisense, GTGATGTTCTCCTCCACCGT (position rat 2622); SUR2 (accession No. D86038) sense, GAGACGGAAGACATTGCCAT (position 2148), antisense, CTATGATCCAGTCAGCGTGC (position 2802); SUR2A/B sense, TGGTCGACATATTTGACGGA (position 4237), antisense, CTCCACACAGAAATCCGTCA (position 5076 and 4900 for SUR2A and SUR2B, respectively); TH (accession No. M69200) sense, CACCTGGAGTACTTTGTGCG (position 387), antisense, CCT-GTGGGTGGTACCCTATG (position 1525); Girk2 (accession No. U11859) sense, CCTACCGATACCTGACGGAC (position 711), antisense, GGGTGCTGGTCTCATAGGTC (position 1580); GFAP (accession No. K01347) sense, AGAACAACCTGGCTGCGTAT (position 407), antisense CTCACATCACCACGTCCTTG (position 1213); GAD67 (accession No. Z49976) sense, TGACATCGACTGCCAATACC (position 731), antisense, GGGTTAGAGATGACCATCCG (position 1835). First multiplex-PCR was performed as hot start in a final volume of 100 µl containing the 10 µl reverse transcription reaction, 100 pmol of each primer, 0.2 mM each dNTP (Pharmacia), 1.8 mM MgCl$_2$, 50 mM KCl, 20 mM Tris–HCl (pH 8.4) and 3.5 U of *Taq* polymerase (Gibco-BRL) in a Perkin Elmer Thermal Cycler 480C with the following cycling protocol: after 3 min at 94°C, 35 cycles (94°C, 30 s; 58°C, 60 s; 72°C, 3 min) of PCR were performed followed by a final elongation period of 7 min at 72°C. The nested-PCR amplifications were carried out in eight individual reactions, in each case with 2.5 µl of the first PCR product under similar conditions with the following modifications: 50 pmol of each primer, 2.5 U of *Taq* polymerase, 1.5 mM MgCl$_2$ and a shorter extension time (60 s) using the following primer pairs: Kir6.2 sense, GCTGCATCTTCATGAAAACG (position 625), antisense, TTGGAGT-CGATGACGTGGTA (position 922); Kir6.1 sense, GCACACAAGAA-CATCCGAGA (position 339), antisense, GGCTGAAAATCAGC-GTCTCT (position 786); SUR1 sense, TCAAGGTTGTGAACCGCA-(position rat 2186), antisense, GGTTTCTGAGATGCGTAGGC-(position rat 2586); SUR2 sense, GGAGACCAAACTGAAATCGG (position 2550), antisense, TGCGTCACAAGAACAACCG (position 2764); SUR2A/B sense, CTTAGATGCCACTGTCACC (position 4463), antisense, ACATGTCTGCACGGACAAAC (position 4976(SUR2A)/4800(SUR2B)); TH sense, TGCACACAGTACATCCGTCA (position 936), antisense, TCTGACACGAAGTACACCGG (position 1312); Girk2 sense, AGACAGAAACCACCATCGGT (position 936), antisense, GA-ACCCGTCTTCCATCGTTA (position 1531); GFAP sense, AGAAAG-GTTGAATCGCTGGA (position 472), antisense, CCAGGGCTA-GCTTAACGTTG (position 988); GAD67 sense, CATATGAAATTGC-ACCCGTG (position 761), antisense, CGGTGTCATAGGAGAC-GTCA (position 1462). To investigate the presence and size of the amplified fragments, 15 µl aliquots of PCR products were separated and visualized in an ethidium bromide-stained agarose gel (2%) by electrophoresis. The predicted sizes (bp) of the eight PCR-generated fragments were: 215 (SUR2), 337 or 513 (SUR2B and SUR2A, respectively), 298 (Kir6.2), 377 (TH), 401 (SUR1), 448 (Kir6.1), 517 (GFAP), 595 (Girk2) and 702 (GAD67). All individual PCR products were verified several times (n >3) by direct sequencing or by subcloning and sequencing.

RNA isolation and cDNA preparation for control reactions

Poly(A)$^+$ RNA was prepared from fresh ventral midbrain and heart of 13-day-old C57Bl/6J mice using the Micro-FastTrack™ Kit (Invitrogene). The reverse transcription was performed with 500 ng of poly(A)$^+$ RNA as described above. For the positive controls carried out in parallel with each single-cell amplification, the resulting midbrain cDNA stock was diluted 1000-fold and 1 µl was used as template for the PCR. All eight PCR fragments were detected routinely in the positive control with the PCR protocol described above. Negative controls were carried out in parallel to single-cell experiments excluding only the harvesting proceedure, and resulted in no detectable bands. To probe for possible amplification of genomic DNA from the harvested single nuclei, in particular from the intronless Kir6.2 gene, single-cell mPCR amplifications were carried out without prior reverse transcription. For all analysed neurons ($n = 10$), no PCR products were detectable. All other primer pairs were designed to be intron spanning.

Acknowledgements

References

Aguilar-Bryan,L. *et al.* (1995) Cloning of the beta cell high-affinity sulfonylurea receptor: a regulator of insulin secretion. *Science*, **268**, 423–426.

Aguilar-Bryan,L., Clement,J.,IV, Gonzalez,G., Kunjilwar,K., Babenko,A. and Bryan,J. (1998) Towards understanding the assembly and structure of KATP channels. *Physiol. Rev.*, **78**, 227–245.

Ashcroft,F.M. (1988) Adenosine 5′-triphosphate-sensitive potassium channels. *Annu. Rev. Neurosci.*, **11**, 97–118.

Ashcroft,F.M. and Gribble,F.M. (1998) Correlating structure and function in ATP-sensitive K$^+$ channels. *Trends Neurosci.*, **21**, 288–294.

Audinat,E., Lambolez,B. and Rossier,J. (1996) Functional and molecular analysis of glutamate-gated channels by patch-clamp and RT–PCR at the single cell level. *Neurochem. Int.*, **28**, 119–136.

Babenko,A., Aguilar-Bryan,L. and Bryan,J. (1998) A view of SUR/KIR6.X, KATP channels. *Annu. Rev. Physiol.*, **60**, 667–687.

Bayer,S.A., Wills,K.V., Triarhou,L.C., Verina,T., Thomas,J.D. and Ghetti,B. (1995) Selective vulnerability of late-generated dopaminergic neurons of the substantia nigra in weaver mutant mice. *Proc. Natl Acad. Sci. USA*, **92**, 9137–9140.

Beal,M. (1996) Mitochondria, free radicals and neurodegeneration. *Curr. Opin. Neurobiol.*, **6**, 661–666.

Brady,P.A., Alekseev,A.E. and Terzic,A. (1998) Operative condition-dependent response of cardiac ATP-sensitive K$^+$ channels towards sulphonylureas. *Circ. Res.*, **82**, 272–278.

Brenner,M. (1994) Structure and transcriptional regulation of the GFAP gene. *Brain Pathol.*, **4**, 245–257.

Bryan,J. and Aguilar-Bryan,L. (1997) The ABCs of ATP-sensitive potassium channels: more pieces of the puzzle. *Curr. Opin. Cell Biol.*, **9**, 553–559.

Cauli,B., Audinat,E., Lambolez,B., Angulo,M., Ropert,N., Tsuzuki,K., Hestrin,S. and Rossier,J. (1997) Molecular and physiological diversity of cortical nonpyramidal cells. *J. Neurosci.*, **17**, 3894–3906.

Chutkow,W., Simon,M., Le Beau,M. and Burant,C. (1996) Cloning, tissue expression and chromosomal localization of SUR2, the putative drug-binding subunit of cardiac, skeletal muscle and vascular KATP channels. *Diabetes*, **45**, 1439–1445.

Clement,J.P.,III, Kunjilwar,K., Gonzalez,G., Schwanstecher,M., Panten,U., Aguilar-Bryan,L. and Bryan,J. (1997) Association and stoichiometry of K (ATP) channel subunits. *Neuron*, **18**, 827–838.

Condé,H. (1992) Organisation and physiology of the substantia nigra. *Exp. Brain Res.*, **88**, 233–248.

Dunn-Meynell,A.A., Routh,V.H., McArdle,J.J. and Levin,B.E. (1997) Low-affinity sulfonylurea binding sites reside on neuronal cell bodies in the brain. *Brain Res.*, **745**, 1–9.

Fujimura,N., Tanaka,E., Yamamoto,S., Shigemori,M. and Higashi,H. (1997) Contribution of ATP-sensitive potassium channels to hypoxic hyperpolarization in rat hippocampal CA1 neurons *in vitro*. *J. Neurophysiol.*, **77**, 378–385.

Gaspar,P., Ben Jelloun,N. and Febvret,A. (1995) Sparing of the dopaminergic neurons containing calbindin-D28k and of the dopaminergic mesocortical projections in weaver mutant mice. *Neuroscience*, **61**, 293–305.

Grace,A. and Onn,S.-P. (1989) Morphology and electrophysiological properties of immunocytochemically identified rat dopamine neurons recorded *in vitro*. *J. Neurosci.*, **9**, 3463–3481.

Graybiel,A.M., Ohta,K. and Roffler-Tarlov,S. (1990) Patterns of cell and fiber vulnerability in the mesostriatal system of the mutant mouse weaver. I. Gradients and compartments. *J. Neurosci.*, **3**, 720–733.

Gribble,F.M., Ashfield,R., Ammala,C. and Ashcroft,F.M. (1997) Properties of cloned ATP-sensitive K$^+$ currents expressed in *Xenopus* oocytes. *J. Physiol.*, **498**, 87–98.

Gribble,F.M., Tucker,S., Seino,S. and Ashcroft,F.M. (1998) Tissue specificity of sulphonylureas: studies on cloned cardiac and β-cell K (ATP) channels. *Diabetes*, **47**,1412–1418.

Hanna,M. and Bhatia,K. (1997) Movement disorders and mitochondrial dysfunction. *Curr. Opin. Neurol.*, **10**, 351–356.

Hirsch,E., Faucheux,B., Damier,P., Mouatt-Prigent,A. and Agid,Y. (1997) Neuronal vulnerability in Parkinson's disease. *J. Neural Transm.*, **50**, 79–88.

Inagaki,N., Gonoi,T., Clement,J.P.,III, Namba,N., Inazawa,J., Gonzalez,G., Aguilar-Bryan,L., Seino,S. and Bryan,J. (1995a) Reconstitution of IKATP: an inward rectifier subunit plus the sulfonylurea receptor. *Science*, **270**, 1166–1170.

Inagaki,N., Tsuura,Y., Namba,N., Masuda,K., Gonoi,T., Horie,M., Seino,Y., Mizuta,M. and Seino,S. (1995b) Cloning and functional characterization of a novel ATP-sensitive potassium channel ubiquitously expressed in rat tissues, including pancreatic islets, pituitary, skeletal muscle and heart. *J. Biol. Chem.*, **270**, 5691–5694.

Inagaki,N., Gonoi,T., Clement,J.P.,III, Wang,C.Z., Aguilar-Bryan,L., Bryan,J. and Seino,S. (1996) A family of sulfonylurea receptors determines the pharmacological properties of ATP-sensitive K$^+$ channels. *Neuron*, **16**, 1011–1017.

Isomoto,S. and Kurachi,Y. (1997) Function, regulation, pharmacology and molecular structure of ATP-sensitive K channels in the cardiovascular system. *J. Cardiovasc. Electrophysiol.*, **8**, 1431–1446.

Isomoto,S., Kondo,C., Yamada,M., Matsumoto,S., Higashiguchi,O., Horio,Y., Matsuzawa,Y. and Kurachi,Y. (1996) A novel sulfonylurea receptor forms with BIR (Kir6.2) a smooth muscle type ATP-sensitive K$^+$ channel. *J. Biol. Chem.*, **271**, 24321–24324.

Iwata,N., Kobayashi,K., Sasaoka,T., Hikada,H. and Nagatsu,T. (1992) Structure of the mouse tyrosine hydroxylase gene. *Biochem. Biophys. Res. Commun.*, **182**, 348–354.

Johnson,S. and North,R. (1992) Two types of neurones in the rat ventral tegmental area and their synaptic inputs. *J. Physiol.*, **450**, 455–468.

Jonas,P., Racca,C., Sakmann,B., Seeburg,P. and Monyer,H. (1994) Differences in Ca^{2+} permeability of AMPA-type glutamate receptor channels in neocortical neurons caused by differential GluR-B subunit expression. *Neuron*, **12**, 1281–1289.

Karschin,A., Brockhaus,J. and Ballanyi,K. (1998) KATP channel formation by SUR1 receptors with Kir6.2 subunits in rat dorsal vagal neurons *in situ*. *J. Physiol.*, **509**, 339–346.

Lacey,M., Mercuri,N. and North,R. (1989) Two cell types in rat substantia nigra zona compacta distinguished by membrane properties and the actions of dopamine and opiods. *J. Neurosci.*, **9**, 1233–1241.

Lee,K., Dixon,A., Freeman,T. and Richardson,P. (1998) Identification of an ATP-sensitive potassium channel current in rat striatal cholinergic interneurones. *J. Physiol.*, **510**, 441–453.

Lesage,F., Duprat,F., Fink,M., Gillemare,E., Coppola,T., Lazdunski,M. and Hugnot,J.-P. (1994) Cloning provides evidence for a familiy of inward rectifier and G-protein coupled K$^+$ channels in the brain. *FEBS Lett.*, **353**, 37–42.

Mercuri,N., Bonci,A., Johnson,S., Stratta,F., Calibresi,P. and Bernadi,G. (1994) Effects of anoxia on rat midbrain dopamine neurons. *J. Neurophysiol.*, **71**, 1165–1173.

Monyer,H. and Lambolez,B. (1995) Molecular biology and physiology at the single-cell level. *Curr. Opin. Neurobiol.*, **5**, 382–387.

Nelson,E., Liang,C., Sinton,C. and German,D. (1996) Midbrain dopaminergic neurons in the mouse: computer-assisted mapping. *J. Comp. Neurol.*, **369**, 361–371.

Okuyama,Y. *et al.* (1998) The effects of nucleotides and potassium channel openers on the SUR2A/Kir6.2 complex K$^+$ channel expressed in a mammalian cell line, HEK293T cells. *Pflügers Arch.*, **435**, 595–603.

O'Dowd,D. and Smith,M. (1996) Single-cell analysis of gene-expression in the nervous system. Measurements at the edge of chaos. *Mol. Neurobiol.*, **13**, 199–211.

Patil,N., Cox,D.R., Bhat,D., Faham,M., Myers,R.M. and Peterson,A.S. (1995) A potassium channel mutation in weaver mice implicates membrane excitability in granule cell differentiation. *Nature Genet.*, **11**, 126–129.

Quale,J., Nelson,M. and Standen,N. (1997) ATP-sensitive and inwardly rectifying potassium channels in smooth muscle. *Physiol. Rev.*, **77**, 1165–1232.

Richards,C.T.S. and Kitai,S. (1997) Electrophysiological and immunocytochemical characterization of GABA and dopamine neurons in the substantia nigra of the rat. *Neuroscience*, **80**, 545–557.

Roeper,J. and Ashcroft,F.M. (1995) Metabolic inhibition and low internal ATP activate K-ATP channels in rat dopaminergic substantia nigra neurons. *Pflügers Arch.*, **430**, 44–54.

Sakura,H., Ammala,C., Smith,P.A., Gribble,F.M. and Ashcroft,F.M. (1995) Cloning and functional expression of the cDNA encoding a novel ATP-sensitive potassium channel subunit expressed in pancreatic β-cells, brain, heart and skeletal muscle. *FEBS Lett.*, **377**, 338–344.

Schreiber,S. and Baudry,M. (1995) Selective vulnerability in the hippocampus—a role for gene expression. *Trends Neurosci.*, **18**, 446–451.

Schwanstecher,C. and Panten,U. (1993) Tolbutamide- and diazoxide-sensitive K$^+$ channels in neurons of the substantia nigra pars reticulata. *Naunyn-Schmiedebergs Arch. Pharmacol.*, **348**, 113–117.

Seutin,V., Shen,K.-Z., North,R. and Johnson,S. (1996) Sulphonylurea-sensitive potassium current evoked by sodium-loading in rat midbrain dopamine neurons. *Neuroscience*, **71**, 709–719.

Spanswick,D., Smith,M., Groppi,V., Logan,S. and Ashford,M. (1997) Leptin inhibits hypothalamic neurons by activation of ATP-sensitive potassium channels. *Nature*, **390**, 521–525.

Stanford,I. and Lacey,M. (1995) Regulation of potassium conductance in rat midbrain dopamine neurons by intracellular adenosine triphosphate (ATP) and the sulphonylureas tolbutamide and glibenclamide. *J. Neurosci.*, **15**, 4651–4657.

Stanford,I. and Lacey,M. (1996) Electrophysiological investigation of adenosine trisphosphate-sensitive potassium channels in the rat substantia nigra pars reticulata. *Neuroscience*, **74**, 499–509.

Stuart,G., Dodt,H.-U. and Sakmann,B. (1993) Patch-clamp recordings from the soma and dendrites of neurons in brain slices using infrared video microscopy. *Pflügers Arch.*, **423**, 511–518.

Surmeier,D., Song,W.-J. and Yan,Z. (1996) Coordinated expression of dopamine receptors in neostriatal medium spiny neurons. *J. Neurosci.*, **16**, 6579–6591.

Szabó,G., Katarova,Z., Körtvély,E., Greenspan,R. and Urbán,C. (1996) Structure and the promotor region of the mouse gene encoding the 67-kD form of glutamic acid decarboxylase. *DNA Cell Biol.*, **15**, 1081–1091.

Trapp,S. and Ballanyi,K. (1995) KATP channel mediation of anoxia-induced outward current in rat dorsal vagal neurons *in vitro. J. Physiol.*, **487**, 37–50.

Verney,C., Febvret-Muzerelle,A. and Gaspar,P. (1995) Early postnatal changes of the dopaminergic mesencephalic neurons in the weaver mutant mouse. *Brain Res. Dev. Brain. Res.*, **89**, 115–119.

Watts,A., Hicks,G. and Henderson,G. (1995) Putative pre- and postsynaptic ATP-sensitive potassium channels in the rat substantia nigra *in vitro. J. Neurosci.*, **15**, 3065–3074.

Yamada,M., Isomoto,S., Matsumoto,S., Kondo,C., Shindo,T., Horio,Y. and Kurachi,Y. (1997) Sulphonylurea receptor 2B and Kir6.1 form a sulphonylurea-sensitive but ATP-insensitive K$^+$ channel. *J. Physiol.*, **499**, 715–720.

Yokoshiki,H., Sunagawa,M., Seki,T. and Sperelakis,N. (1998) ATP-sensitive K$^+$ channels in pancreatic, cardiac and vascular smooth muscle cells. *Am. J. Physiol.*, **274**, C25–C37.